Biosensors and Bioelectronics 38 (2012) 31–36

Contents lists available at SciVerse ScienceDirect

Biosensors and Bioelectronics

journal homepage: www.elsevier.com/locate/bios

A graphene oxide based biosensor for microcystins detection by fluorescence resonance energy transfer

Yan Shi [a,b,1], Jiazhen Wu [a,b,1], Yujing Sun [a,b], Yue Zhang [a,b], Zhiwei Wen [a,b], Haichao Dai [a,b], Hongda Wang [a,b], Zhuang Li [a,b,*]

[a] State Key Laboratory of Electroanalytical Chemistry, Changchun Institute of Applied Chemistry, Chinese Academy of Sciences, Changchun, 130022, Jilin, PR China
[b] Graduate School of the Chinese Academy of Sciences, Beijing 100039, PR China

ARTICLE INFO

Article history:
Received 9 February 2012
Received in revised form
21 April 2012
Accepted 24 April 2012
Available online 7 June 2012

Keywords:
Microcystin
Graphene oxide
Fluorescence resonance energy transfer
Gold nanoparticle
Biosensor

ABSTRACT

Water safety is one of the most pervasive problems afflicting people throughout the world. Microcystin, a hepatotoxin produced by cyanobacteria, poses a growing and serious threat of water safety. According to World Health Organization (WHO), the limit of content of microcystin-LR (MC-LR) in drinking water is as low as 1 μg/L; it is thus necessary to explore a sensitive method for the trace detection of microcystins (MCs). Based on the observation of gold nanoparticles (Au NPs) induced graphene oxide (GO) fluorescence quenching, a reliable biosensor was developed here for microcystins detection. MCs could be attached on Au NPs through the interaction with single strand-DNA (ss-DNA) modified on Au NPs, which formed Au–DNA–MCs complexes. These MCs in the complexes could be immunologically recognized by the antibodies adsorbed on GO sheets, as a result, Au NPs were close enough to quench the photoluminescence of GO by the fluorescence resonance energy transfer (FRET). The fluorescence intensity decreased with the increase of MCs as more Au NPs linked onto GO surface. The limit of detection was 0.5 and 0.3 μg/L for microcystin-LR and microcystin-RR (MC-RR), respectively, which satisfies the strictest standard of WHO. Well defined results were also obtained in natural lake water and the specificity experiment. The antibody used here could recognize Adda group, the conservative part of MCs, which allowed the biosensor to detect both single toxin and the total content of MCs existing in the water sample.

1. Introduction

Microcystins (MCs), one of the most dangerous toxins produced by cyanobacteria from diverse natural environments, pose a growing and serious threat in water supplies throughout the world (Loyprasert et al., 2008; Pyo and Shin, 1999). MCs mainly inhibit the activity of protein serine/threonine phosphatases in the protein phosphatase (PPP) family and seriously affect the cellular signaling (Cass et al., 2003), which present as potent and highly specific hepatotoxins and also are suspected as a threat of brain, kidney and colon (Alverca et al., 2009; Fischer et al., 2005; Zegura et al., 2008). Up to now, MCs have caused deaths in both animals and humans in many countries, such as Australia, China, and Brazil (dos Anjos et al., 2006; Francis, 1878; Xu et al., 2000; Yu, 1995).

The structure of MCs is a kind of monocyclic heptapeptide, as displayed in Fig. 1A. Variants of MCs, like microcystin-LR (MC-LR) and microcystin-RR (MC-RR), were classified by the two L-amino acids in X and Z positions (ellipses in Fig. 1A) (Al Momani et al., 2008). Adda group (3-amino-9-methoxy-2, 6, 8-trimethyl-10-phenyldeca-4, 6-dienoic acid) (square bracket in Fig. 1A) is the unique feature of MCs, which plays an important role in their toxicity (Campas and Marty, 2007; Namikoshi et al., 1992).

From 1998, World Health Organization (WHO) established the guideline level of MC-LR in drinking water less than 1 μg/L (Paulino et al., 2009), which promoted researchers to seek different methods and materials on the trace detection of MC-LR, such as the chlorophyll fluorescence analysis (Saqrane et al., 2009), the liquid chromatography (Weller et al., 2001) or coupled with mass spectrometry (LC–MS) method (Furey et al., 2007), and the protein phosphatase-2A (PP2A) inhibition assay (Campas et al., 2005; Cass et al., 2003). Carbon materials were also used in the analysis process of MCs because of their excellent conductive property. For example, Xu et al. (2009) developed a paper sensor based on single-walled carbon nanotubes (SWNT), and Zhang et al. (2011) constructed an immunosensor by the assembly of gold nanoparticles on nitrogen-doped carbon nanotubes.

Emerging as a new carbon material, graphene and its derivates have drawn a lot of attentions, including biological detection

* Corresponding author at: State Key Laboratory of Electroanalytical Chemistry, Changchun Institute of Applied Chemistry, Chinese Academy of Sciences, Changchun, 130022 Jilin, PR China. Tel./fax: +86 431 526 2057.
E-mail address: zli@ciac.jl.cn (Z. Li).
[1] The two authors contributed equally to this paper.

0956-5663/$ - see front matter Crown Copyright © 2012 Published by Elsevier B.V. All rights reserved.
http://dx.doi.org/10.1016/j.bios.2012.04.053

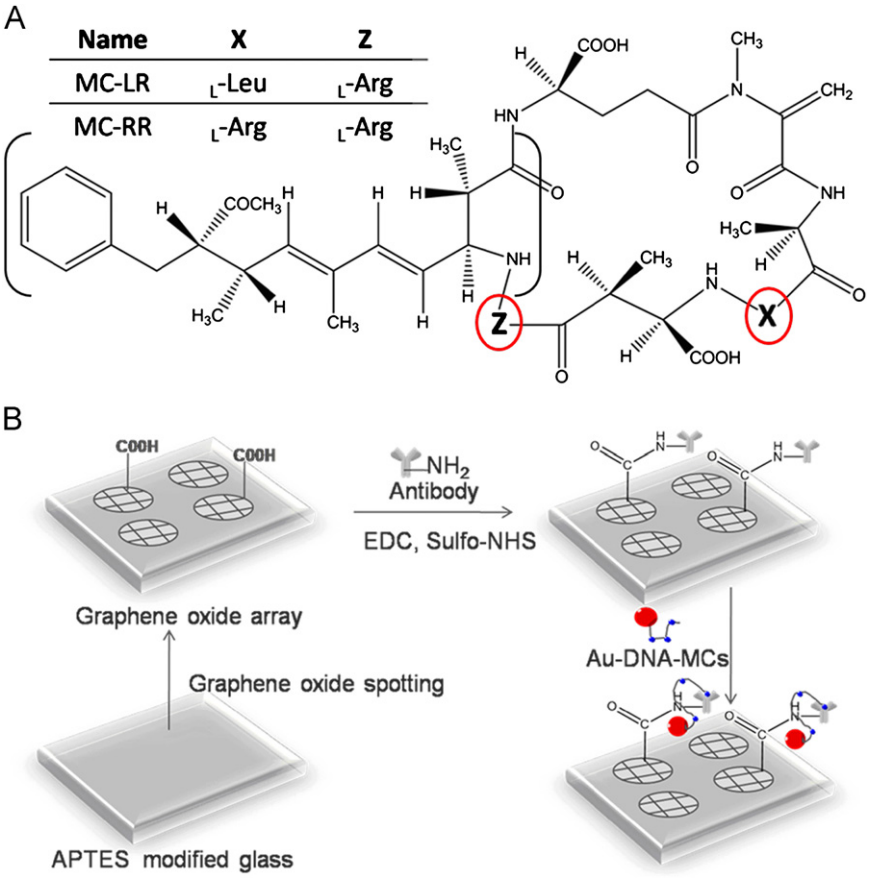

Fig. 1. (A) Chemical structure of microcystins and the different amino acids in X and Z positions (ellipses) for MC-LR and MC-RR, and Adda group was marked with square bracket. (B) Illustration of GO based fluorescence biosensor.

(Zhao et al., 2011; Jiang et al., 2010), microelectrical devices fabrication (Gilje et al., 2007), and nanocomposites synthesis (Stankovich et al., 2006; Xu et al., 2008). Graphene oxide (GO) shows a great potential in biological applications (Mohanty and Berry, 2008; Yan and Chen, 2011) because it can be dispersed in aqueous solution uniformly and remains the properties, such as simple chemical functionalization, fluorescence quenching phenomenon, and intrinsic photoluminescence (He et al., 2010; Lu et al., 2009). In the process of GO preparation, chemical oxidization occurs in the two-dimensional crystal structure of graphite, some carbon atoms are sp^3 hybridized and covalently bonded with oxygen in the form of epoxy and hydroxyl groups. The geminate recombination of local electron–hole pairs in sp^3 clusters embedded in the sp^2 matrix can act as the luminescence centers or chromophores (Eda et al., 2010). Based on this fluorescence property, Seo's group employed GO as an efficient fluorescent label for the detection of DNA hybridization and pathogen by fluorescence resonance energy transfer (FRET) (Jung et al., 2010; Liu et al., 2010).

Taking the advantage of FRET and immunorecognition, we developed a reliable biosensor for the trace detection of MCs with the fluorescence property of GO. Graphene oxide sheets were deposited on a positively charged glass slide in an array format, and then covalently linked with the antibody of MCs (Adda group). The complex of Au NPs and MCs linked by ss-DNA is used for the immobilization of MCs. Once the specific interactions occurred between these MCs and their antibodies adsorbed on GO array, Au NPs could approach to GO surface, which induced the quenching of GO fluorescence by FRET between GO and Au NPs. Rapid, precise, and trace detection of MCs were owing to the fast response of FRET process and the specific recognition of the antibody.

2. Materials and methods

2.1. Reagents

MCs (MC-LR, MC-RR), shellfish poisons (saxitoxin (STX), neosaxitoxin (NEO)) and the antibody special to Adda group of MCs were purchased from Express Technology Co., Ltd. (Beijing, China). DNA oligonucleotides (A_{15}, T_{15} and SH-A_{15}) were synthesized by Sangon Biotech Co., Ltd. (Shanghai, China) and used without further purification. 1-Ethyl-3-[3-dimethylaminopropyl] carbodiimide hydrochloride (EDC), N-hydroxy sulfosuccinimide (Sulfo-NHS), (3-aminopropyl) triethoxysilane (APTES) and N, N-diisopropylethylamine were bought from Sigma-Aldrich (USA).

2.2. Antibodies modified GO array fabrication

Positively charged glass slides modified by APTES were carried out using the method according to Lindsay's work (Lohr et al., 2007). In short, a vacuum desiccator was purged with argon for 2 min, and then 30 μL of APTES and 15 μL of N, N-diisopropylethylamine were dropped into two small containers at the bottom of the vacuum desiccator with argon for a further 3 min. After placing clean glass slides at the bottom of the vacuum desiccator, the desiccator was purged for another 3 min and then sealed off to leave the glass slides exposed to APTES vapor. After 2 h, APTES was removed, and the treated glass slides were stored in the sealed desiccator until needed.

A water-soluble GO was prepared by using a modified Hummer's method (Hummers and Offeman, 1958). 1 μL as-prepared GO sheets (0.05 mg/mL) were adsorbed on the APTES modified

glass slide as array format by electrostatic force and dried in a humid chamber. After washing with ultrapure water and dried in N_2, 1 μL EDC (15 mM) and NHS (30 mM) were added and incubated for 30 min at 37 °C to activate the carboxyl group of GO, then washed to remove the excess part. A solution of MCs antibody (1 μL, 1 ng/μL) was incubated on the same spot for 3 h to enable the covalent linkage on the GO surface.

2.3. Au–DNA–MC complex preparation

The ss-DNA (15 mer: 5′-SH AAA AAA AAA AAA AAA-3′) labeled Au NPs (13 nm) was synthesized according to Dong's method with a minor modification (Du et al., 2009; Li et al., 2009). Firstly, a sodium citrate solution (0.1 M, 1.94 mL) was rapidly added to a boiled $HAuCl_4$ aqueous solution (50 mL H_2O, 0.167 mL 10% $HAuCl_4$) under vigorous stirring. The mixed solution was boiled for 40 min and the obtained wine-red gold sol was cooled to room temperature under mild stirring. Then, 3 mL of as-prepared Au NPs solution was transferred to a clean glass vials, and incubated with 20 μL, 10 μM ss-DNA (HS-A_{15}). After 24 h magnetic stirring of reaction and stabilization, the obtained Au–DNA solution was centrifuged at 13,000 rpm under room temperature for 15 min twice to remove the free DNA. The Au–DNA (about 10 nM) was stored in the phosphate buffer (PB) solution (5 mM PB, 0.1 M NaCl, pH = 7) for further use. The final Au–DNA–MCs complex was formed by mixing MCs and Au–DNA solution. The final concentration of Au–DNA is 0.5 nM, and the concentration of MCs is from 10^{-4} to 2.5 μg/L. The interactions among Au NPs, DNA and MCs were monitored by UV absorption spectra with a Cary 50 Bio UV–visible spectrophotometer.

2.4. Detection of MC-LR and MC-RR

On the antibody modified GO sheets, 1 μL Au–DNA–MCs complexes were added and incubated for 3 h, 37 °C in humid chamber to make sure that Au–DNA–MCs complexes link the target antibody, and the Au NPs get close to the GO surface. The samples were then measured for scanning fluorescence images using a Leica TCS SP2 Confocal Microscope with excitation wavelength of 534 nm (PMT detector voltage = 800 V). Negative control (NC) of the fluorescence quenching experiment was operated as Au–DNA conjugated Ab–GO with treatment of T_{15} (15-mer of thymine: 5′-TTT TTT TTT TTT TTT-3′), explained in Section 3. To simulate the detection in polluted water, the samples of lake water were made by adding different concentrations of MCs standard solution into lake water, and then incubated with Au–DNA, forming Au–DNA–MCs complexes for the MCs detection.

2.5. AFM measurement for the characterization of the sensor

AFM was used to characterize the morphology of the sensor at each functionalizing step, including GO sheets adsorbed on APTES-modified glass slides, antibodies (Ab) functionalized GO sheets, morphological change after the addition of MC-LR, and the Au NPs adsorption due to the specific interactions between MC-LR and its antibody. AFM experiments were carried out with Dimension Icon (Veeco Instruments, USA) in tapping mode, scanning the samples used in fluorescence quenching experiments. All AFM images showed the topography and were raw data except for flattened using a standard algorithm within the Nanoscope software to remove artificial height offsets between consecutive scan lines of the raw images.

3. Results and discussion

3.1. Mechanism of GO array sensor for MCs sensing

The scheme of MCs sensing on a GO array is illustrated in Fig. 1B. GO was fabricated from the chemical oxidization of graphite, and could be dispersed uniformly in water as the colloidal suspension of small sheets. During the oxidization process of GO synthesis, oxygen-containing groups were introduced on GO surface, including carboxylic acids, hydroxyl group and epoxides, which resulted in the negative charge on the homogenous GO surface in solution (Stankovich et al., 2007). These GO sheets then self-assemble onto a positively charged glass slide modified by APTES, which were well retained even after the washing step (Liu et al., 2010). The following antibodies for MCs (Adda group) were immobilized on the GO array by a carbodiimide-assisted amidation reaction with EDC and NHS (Jung et al., 2010). When the target MCs molecules were captured by their antibodies on the GO array, the fluorescence of GO would be quenched by Au NPs linked with MCs because of FRET. Through measuring the fluorescence decrease, MCs can be detected sensitively and quantitatively.

To realize the GO based fluorescence biosensor, the interactions between Au NPs, DNA and MCs were firstly confirmed. In our previous work, we proved that MC-LR bound with plasmid DNA in the minor groove, and could also interact with DNA bases, especially with adenine and thymine (Shi et al., 2011). Here, the interaction between MCs and DNA oligonucleotide was further studied by UV spectra (Fig. 2A). It was found that, in the presence of A_{15}, the absorbance of MCs increased with a red shift, which indicated the binding between MCs and A_{15}. Besides that, a small peak shift at 520 nm and the characteristic absorption band near 270 nm of HS-A_{15} after the mixing of HS-A_{15} and Au NPs certified the formation of Au–DNA complex (Fig. 2B) (Liu et al., 2010). This

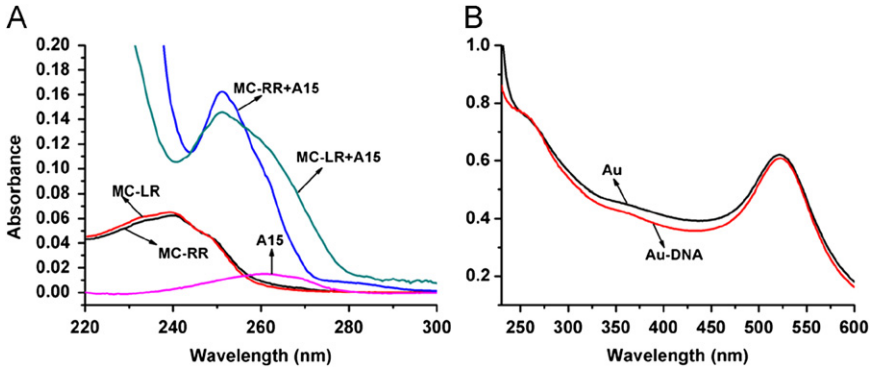

Fig. 2. UV spectra of (A) MC-LR, MC-RR, A_{15} and the products after their binding, (B) Au NPs (13 nm) and complex after DNA modified.

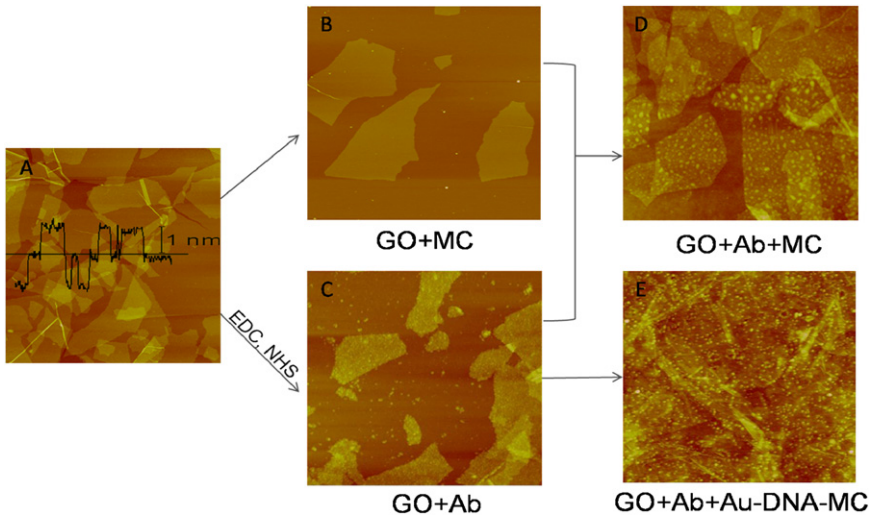

Fig. 3. AFM images for each step of the GO based fluorescence biosensor. (A) The pristine GO array with 1 nm difference in height between layers. (B) GO sheets with MC-LR added. (C) GO array with antibody immobilization in the presence of EDC and NHS. (D) Height and morphology change after MC-LR adsorbed on Ab–GO surface. (E) Au NPs linked on GO surface through the interaction between Ab and Au–DNA–MC complex. The scale for all images is 5 μm, and Z-range is 10 nm for (A)–(D) and 30 nm for (E).

complex was stored in the phosphate buffer solution with 0.1 M NaCl forming stable red solution, which was another proof for the fabrication of DNA on Au NPs. Then, MCs linked Au NPs, which were bridged with 15-mer ss-DNA (Au–DNA–MCs), were synthesized by mixing MCs with Au–DNA solution. When the Au–DNA–MCs complexes were selectively bound to the antibodies adsorbed on GO array, the decrease of the GO fluorescence was detected for the identification of MCs.

3.2. AFM characterization of biosensor

AFM analysis was performed to obtain the topographical profile for each step during the fabrication of GO based fluorescence biosensor. Fig. 3A shows uniform monolayer and bilayers of GO sheets adsorbed on APTES modified glass slide with 1 nm distance between layers. GO covered almost the entire surface, which prevented the non-specific binding between MCs and the positively charged glass surface. Taking MC-LR as an example, the fabricated steps of the biosensor were characterized by AFM. Firstly, Fig. 3B displays that no MC-LR adsorbed on GO array, which eliminated the effect of non-specific adsorption. Then, in the presence of EDC and NHS, antibodies were adsorbed on GO sheets with large amount, which induced the height increase of the complex (Ab- GO) to about 2 nm (Fig. 3C). Obvious morphological change was observed after the addition of MC-LR onto Ab–GO surface with the height of about 4 nm, which indicated the specific recognition between antibodies and MC-LR in our experiment conditions (Fig. 3D). After Au–DNA–MC-LR complexes reacted with the antibodies, the final complexes on GO array were displayed in Fig. 3E. Large amount of Au NPs and the total height of about 17 nm of the final complexes confirmed that the Au NPs were sufficiently close to the GO surface for FRET detection, which was in the distance of less than 10 nm (Quan et al., 2010; Sebastian and Swathi, 2009).

3.3. Reduction of Au–DNA non-specific adsorption

Au–DNA complex could be also adsorbed on Ab–GO without MCs (Fig. 4A and B) due to the high affinity between GO and ss-DNA, which made the dependent relationship between fluorescence intensity and the MC concentration uncertain. DNA oligonucleotides (T_{15}) were used to eliminate the non-specific adsorption of Au–DNA, based on the different affinity of single and

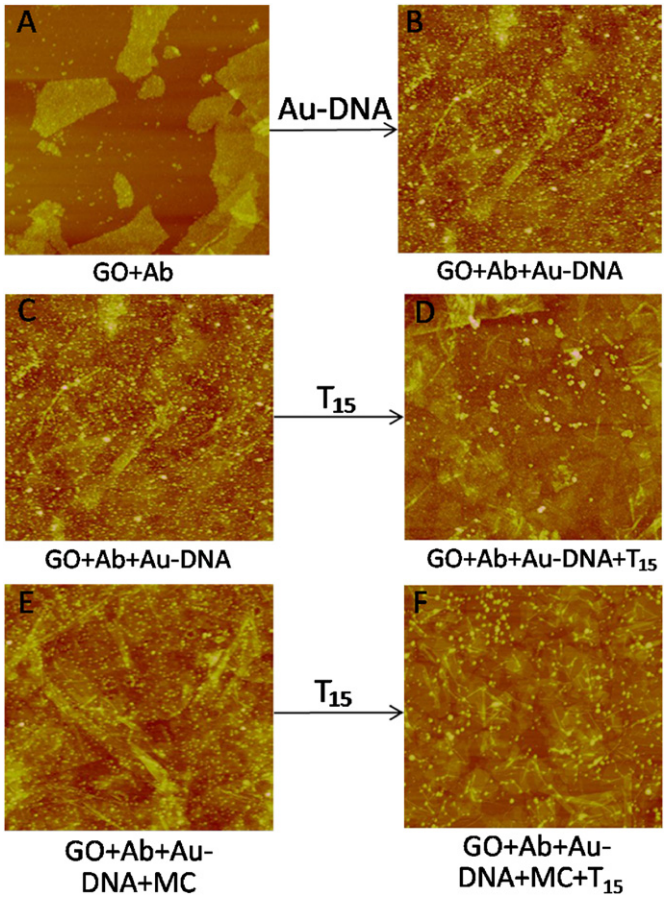

Fig. 4. AFM images of (A) and (B) Ab–GO surfaced treated with Au–DNA complex. (C) and (D) Result after the treatment of T_{15} for the removal of non-specific interaction of Au–DNA. (E) and (F) MC-LR detection without and with the treatment of T_{15}. The scale for all images is 5 μm and Z-range is 30 nm.

double strand DNA on GO array. Binding with complementary strands would disturb the interaction between ss-DNA and GO, resulting in the exfoliation of non-specifically adsorbed ss-DNA (Wu et al., 2011). After the treatment of T_{15}, only a few Au NPs

(small dots on the surfaces) remained on the surface of GO (Fig. 4C and D), which proved the importance of T_{15} treatment. It was also helpful in the detection of MC-LR, shown in Fig. 4E and F. Owing to T_{15} treatment, many non-specifically adsorbed Au–DNA have been removed, and those remained could be considered as the immobilized Au–DNA–MC complexes *via* the immunorecognition between MCs and their antibodies modified on GO layers. To reduce the influence of non-specifically adsorbed Au–DNA, this Au–DNA conjugated Ab–GO surface with T_{15} treatment (Fig. 4D) was chosen as the negative control (NC) for the following fluorescence quenching experiments.

3.4. Detection of MC-LR and MC-RR

The fluorescence emission of GO is caused by the disruption of the fully delocalized π electron system in graphene crystals during the oxidation process, which introduces oxygen-containing groups leading to the localization of the excitation energy at the defect sites (Eda et al., 2010). The unique atomic and electronic structure of GO makes it possible for the recombination of localized e–h pairs in sp^3 clusters, which was considered as the luminescence centers of chromophores (Liu et al., 2010; Yan and Chen, 2011). In this biosensor, GO and Au NPs act as an energy donor and acceptor pair, which leads to the fluorescence quenching of GO through the FRET phenomenon. Fig. 5A displayed the fluorescence scanning image and the relative fluorescence intensity of each reaction step on GO arrays, and MC-LR was chosen as the analyte with the concentration of 1 μg/L. The average fluorescence intensity of pristine GO array was normalized to 1. The adsorption of antibodies and MC-LR made almost no change of GO fluorescence. However, a sharp drop (about $58 \pm 4.8\%$) occurred when Au–DNA complexes were added onto the Ab–GO surface. After the treatment of T_{15}, the fluorescence intensity recovered to $92 \pm 0.9\%$, which reflected the necessity of the T_{15} treatment again. Most of the non-specifically adsorbed Au–DNA complexes were removed by T_{15} treatment, which made the fluorescence intensity recovered, and reduced the error of the results. The complexes of Au–DNA–MCs with different concentrations of MCs, ranging from 10^{-4} to 2.5 μg/L were incubated on the Ab–GO surfaces for MCs detection. As the concentration of MCs increased, the quenching effect became more dominant, resulting in the gradually reduced fluorescence intensity, shown in Fig. 5B and C. The more MCs molecules existed, the more Au NPs were linked onto the Ab–GO surface, and the FRET phenomenon was more significant, leading to the decrease of fluorescence intensity. The average relative fluorescence intensities were measured at each concentration of MCs, and the corresponding quenching efficiencies were calculated as $24 \pm 2.5\%$, $29 \pm 1.7\%$, $41 \pm 1.2\%$, $47 \pm 4.7\%$, $53 \pm 2.1\%$, and $68 \pm 2.4\%$, respectively for MC-LR, and $26 \pm 1.0\%$, $32 \pm 0.6\%$, $42 \pm 4.1\%$, $47 \pm 0.2\%$, $55 \pm 1.9\%$, and $66 \pm 1.8\%$ for MC-RR. Given that the threshold of quenching efficiency would be more than 50% to recognize the MCs molecules (Liu et al., 2010), the calculated limit of detection (LOD) is 0.5 μg/L for MC-LR and 0.3 μg/L for MC-RR, which are comparable with the results obtained in SWNT-paper method (Xu et al., 2009), nonseparation electrochemical enzyme immunoassay (Zhang et al., 2007), and the carbon nanohorn analysis (Ju et al., 2010).

According to WHO requirements, the content of MC-LR in the drinking water should be less than 1 μg/L, and the LOD mentioned above could fulfill this level. This GO based fluorescence biosensor was also used to simulate MCs detection in polluted water samples. Different concentrations of MCs standard solution were added to the lake water samples (South Lake in Changchun, China) without any other treatment. Fig. 6A and B displayed the laser scanning confocal fluorescence images and the relative fluorescence intensity of different concentrations of MCs in the lake water. The results of the fluorescence quenching of both MC-LR and MC-RR were similar with those in ultrapure water, and the quenching efficiency in lake water was slightly larger (about 4%), which was probably caused by the disturbance of other substances in lake water.

To demonstrate the specificity of MCs detection on this biosensor, we performed the detection of shellfish poisons (STX, NEO) following the same procedure as the detection of MCs. Shellfish poisons are another type of toxin produced by cyanobacteria. The concentrations of the toxins used in our experiment were all 1 μg/L, and the fluorescence images and intensities were displayed in Fig. 6C. The unmatched toxins, STX and NEO, did not cause the fluorescence quenching and showed a similar level of fluorescence intensities to the negative control. This high specificity came from the specific interaction between MCs and their antibodies. The antibody used here was specific for Adda group, the conservative part of MCs, which made it possible to detect the total content of MCs in water samples and could meet the requirement of specific MCs detection in polluted water.

4. Conclusions

In summary, we demonstrated that the FRET phenomenon between GO array and Au NPs could be utilized as a high-sensitive

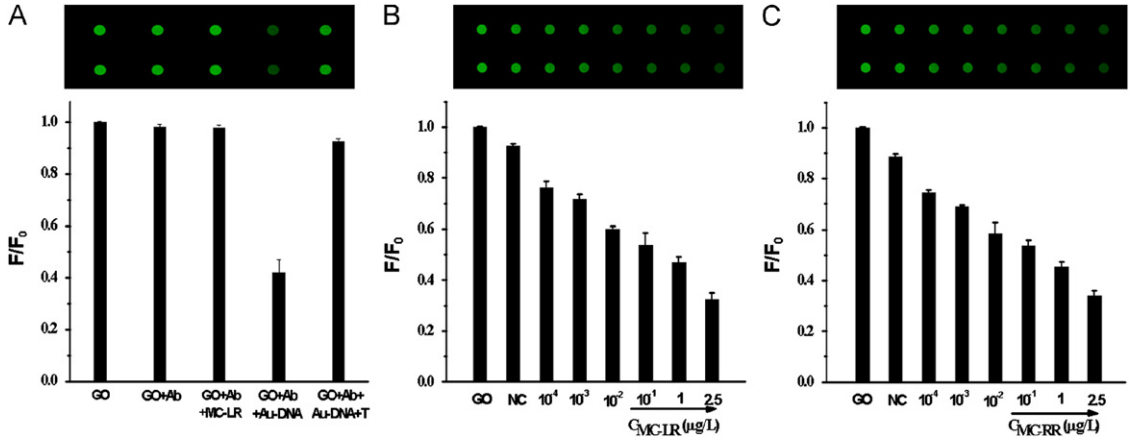

Fig. 5. The laser scanning confocal fluorescence images and relative fluorescence intensity (F) compared to the fluorescence intensity of the pristine GO (F_0) of (A) pristine GO and contract steps, (B) and (C) different concentrations of MCs measured in the GO based fluorescence biosensor, as 10^{-4}, 10^{-3}, 10^{-2}, 10^{-1}, 1, and 2.5 μg/L. The fluorescence intensity difference between pristine GO and the negative control (NC) is about 8%.

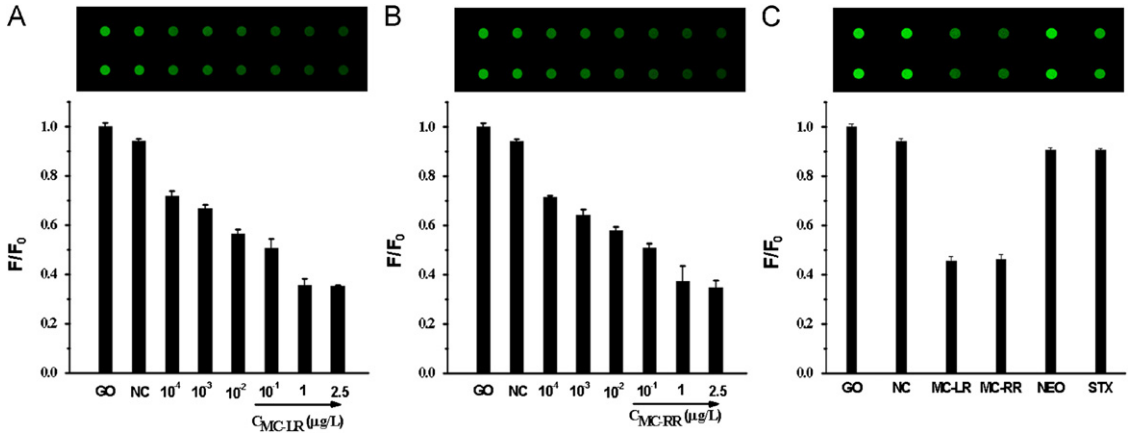

Fig. 6. The laser scanning confocal fluorescence images and relative fluorescence intensity of MCs detection in lake water samples (A) and (B), and the comparison with shellfish poison, STX and NEO, (C). All other conditions were the same as those in Fig. 5. The fluorescence intensity difference between GO and NC is about 6%.

biosensor for trace microcystins' detection to ensure water safety. AFM experiments were used to monitor each step of the biosensor fabrication. Well defined fluorescence quenching signals from MC-LR and MC-RR were obtained in experimental ultrapure water as well as lake water. The LOD of MC-LR and MC-RR were 0.5 and 0.3 μg/L, respectively, which meet the requirement of WHO guideline. This MCs biosensor showed great selectivity and has almost no response to other toxins, such as STX and NEO. This technique is very versatile and can be easily applied to other harmful toxins in water pollution.

Acknowledgment

Financial support by the National Basic Research Program of China (973 program, no. 2010CB933600), the National Natural Science Foundation of China (no. 20775077), and the Chinese Academy of Sciences (no. KJCX2-YW-H11) is gratefully acknowledged.

References

Al Momani, F., Smith, D.W., El-Din, M.G., 2008. Journal of Hazardous Materials 150, 238–249.
Alverca, E., Andrade, M., Dias, E., Bento, F.S., Batoreu, M.C.C., Jordan, P., Silva, M.J., Pereira, P., 2009. Toxicon 54, 283–294.
Campas, M., Marty, J.L., 2007. Biosensors & Bioelectronics 22, 1034–1040.
Campas, M., Szydlowska, D., Trojanowicz, M., Marty, J.L., 2005. Biosensors & Bioelectronics 20, 1520–1530.
Cass, A.E.G., Noble, J.E., Ganju, P., 2003. Analytical Chemistry 75, 2042–2047.
dos Anjos, F.M., Bittencourt-Oliveira, M.D., Zajac, M.P., Hiller, S., Christian, B., Erler, K., Luckas, B., Pinto, E., 2006. Toxicon 48, 239–245.
Du, Y., Li, B.L., Wang, F., Dong, S.J., 2009. Biosensors & Bioelectronics 24, 1979–1983.
Eda, G., Lin, Y.Y., Mattevi, C., Yamaguchi, H., Chen, H.A., Chen, I.S., Chen, C.W., Chhowalla, M., 2010. Advanced Materials 22, 505–509.
Fischer, W.J., Altheimer, S., Cattori, V., Meier, P.J., Dietrich, D.R., Hagenbuch, B., 2005. Toxicology and Applied Pharmacology 203, 257–263.
Francis, G., 1878. Nature 18, 11–12.
Furey, A., Allis, O., Dauphard, J., Hamilton, B., Shuilleabhain, A.N., Lehane, M., James, K.J., 2007. Analytical Chemistry 79, 3436–3447.
Gilje, S., Han, S., Wang, M., Wang, K.L., Kaner, R.B., 2007. Nano Letters 7, 3394–3398.
He, S.J., Song, B., Li, D., Zhu, C.F., Qi, W.P., Wen, Y.Q., Wang, L.H., Song, S.P., Fang, H.P., Fan, C.H., 2010. Advanced Functional Materials 20, 453–459.
Hummers, W.S., Offeman, R.E., 1958. Journal of the American Chemical Society 80, 1339.
Jiang, J.H., Chang, H.X., Tang, L.H., Wang, Y., Li, J.H., 2010. Analytical Chemistry 82, 2341–2346.
Ju, H.X., Zhang, J., Lei, J.P., Xu, C.L., Ding, L., 2010. Analytical Chemistry 82, 1117–1122.
Jung, J.H., Cheon, D.S., Liu, F., Lee, K.B., Seo, T.S., 2010. Angewandte Chemie: International Edition 49, 5708–5711.
Li, B.L., Du, Y., Dong, S.J., 2009. Analytica Chimica Acta 644, 78–82.
Liu, F., Choi, J.Y., Seo, T.S., 2010. Biosensors & Bioelectronics 25, 2361–2365.
Lohr, D., Bash, R., Wang, H., Yodh, J., Lindsay, S., 2007. Methods 41, 333–341.
Loyprasert, S., Thavarungkul, P., Asawatreratanakul, P., Wongkittisuksa, B., Limsakul, C., Kanatharana, P., 2008. Biosensors & Bioelectronics 24, 78–86.
Lu, C.H., Yang, H.H., Zhu, C.L., Chen, X., Chen, G.N., 2009. Angewandte Chemie: International Edition 48, 4785–4787.
Mohanty, N., Berry, V., 2008. Nano Letters 8, 4469–4476.
Namikoshi, M., Rinehart, K.L., Sakai, R., Stotts, R.R., Dahlem, A.M., Beasley, V.R., Carmichael, W.W., Evans, W.R., 1992. Journal of Organic Chemistry 57, 866–872.
Paulino, S., Valerio, E., Faria, N., Fastner, J., Welker, M., Tenreiro, R., Pereira, P., 2009. Hydrobiologia 621, 207–211.
Pyo, D., Shin, H., 1999. Analytical Chemistry 71, 4772–4775.
Quan, X., Liu, M., Zhao, H.M., Chen, S., Fan, X.F., 2010. Chemical Communications 46, 7909–7911.
Saqrane, S., El Ghazali, I., Oudra, B., Bouarab, L., Dekayir, S., Mandi, L., Ouazzani, N., Vasconcelos, V.M., 2009. Toxicon 53, 9–14.
Sebastian, K.L., Swathi, R.S., 2009. Journal of Chemical Sciences 121, 777–787.
Shi, Y., Guo, C.L., Sun, Y.J., Liu, Z.L., Xu, F.G., Zhang, Y., Wen, Z.W., Li, Z.A., 2011. Biomacromolecules 12, 797–803.
Stankovich, S., Dikin, D.A., Piner, R.D., Kohlhaas, K.A., Kleinhammes, A., Jia, Y., Wu, Y., Nguyen, S.T., Ruoff, R.S., 2007. Carbon 45, 1558–1565.
Stankovich, S., Dikin, D.A., Dommett, G.H.B., Kohlhaas, K.M., Zimney, E.J., Stach, E.A., Piner, R.D., Nguyen, S.T., Ruoff, R.S., 2006. Nature 442, 282–286.
Weller, M.G., Zeck, A., Niessner, R., 2001. Analytical Chemistry 73, 5509–5517.
Wu, M., Kempaiah, R., Huang, P.J.J., Maheshwari, V., Liu, J.W., 2011. Langmuir 27, 2731–2738.
Xu, C.L., Wang, L.B., Chen, W., Xu, D.H., Shim, B.S., Zhu, Y.Y., Sun, F.X., Liu, L.Q., Peng, C.F., Jin, Z.Y., Kotov, N.A., 2009. Nano Letters 9, 4147–4152.
Xu, L., Lam, P.K.S., Chen, J., Zhang, Y., Harada, K., 2000. Environmental Toxicology 15, 71–75.
Yan, X.P., Chen, J.L., 2011. Chemical Communications 47, 3135–3137.
Xu, Y.X., Bai, H., Lu, G.W., Li, C., Shi, G.Q., 2008. Journal of the American Chemical Society 130, 5856–5857.
Yu, S.Z., 1995. Journal of Gastroenterology and Hepatology 10, 674–682.
Zegura, B., Volcic, M., Lah, T.T., Filipic, M., 2008. Toxicon 52, 518–525.
Zhang, F.H., Yang, S.H., Kang, T.Y., Cha, G.S., Nam, H., Meyerhoff, M.E., 2007. Biosensors & Bioelectronics 22, 1419–1425.
Zhang, J., Lei, J.P., Pan, R., Leng, C.A., Hu, Z., Ju, H.X., 2011. Chemical Communications 47, 668–670.
Zhao, X.-H., Kong, R.-M., Zhang, X.-B., Meng, H.-M., Liu, W.-N., Tan, W., Shen, G.-L., Yu, R.-Q., 2011. Analytical Chemistry 83, 5062–5066.